

Essential role of the chaperonin folding compartment *in vivo*

Yun-Chi Tang^{1,2}, Hung-Chun Chang^{1,3},
Kausik Chakraborty, F Ulrich Hartl*
and Manajit Hayer-Hartl*

Department of Cellular Biochemistry, Max Planck Institute
of Biochemistry, Martinsried, Germany

The GroEL/GroES chaperonin system of *Escherichia coli* forms a nano-cage allowing single protein molecules to fold in isolation. However, as the chaperonin can also mediate folding independently of substrate encapsulation, it remained unclear whether the folding cage is essential *in vivo*. To address this question, we replaced wild-type GroEL with mutants of GroEL having either a reduced cage volume or altered charge properties of the cage wall. A stepwise reduction in cage size resulted in a gradual loss of cell viability, although the mutants bound non-native protein efficiently. Strikingly, a mild reduction in cage size increased the yield and the apparent rate of green fluorescent protein folding, consistent with the view that an effect of steric confinement can accelerate folding. As shown *in vitro*, the observed acceleration of folding was dependent on protein encapsulation by GroES but independent of GroES cycling regulated by the GroEL ATPase. Altering the net-negative charge of the GroEL cage wall also strongly affected chaperonin function. Based on these findings, the GroEL/GroES compartment is essential for protein folding *in vivo*.

The EMBO Journal (2008) 27, 1458–1468. doi:10.1038/emboj.2008.77; Published online 17 April 2008

Subject Categories: proteins

Keywords: chaperonin; confinement; GroEL; protein folding

Introduction

A subset of cytosolic proteins, including at least 13 essential proteins, are strictly dependent on the chaperonin GroEL and its co-factor GroES for folding (Kerner *et al*, 2005). This likely explains why GroEL and GroES are essential for growth of *E. coli* (Fayet *et al*, 1989). Based on mechanistic studies *in vitro*, GroEL and GroES form a nano-compartment for single protein molecules to fold unimpaired by aggregation

(Mayhew *et al*, 1996; Weissman *et al*, 1996). Moreover, recent experimental and theoretical studies provided evidence that transient enclosure of unfolded protein in the chaperonin cage may alter the folding energy landscape, resulting in accelerated folding for some proteins (Brinker *et al*, 2001; Baumketner *et al*, 2003; Takagi *et al*, 2003; Tang *et al*, 2006; Lucent *et al*, 2007). However, as GroEL/GroES also assists protein folding by a binding-and-release mechanism that is independent of encapsulation, it has remained unclear whether the chaperonin cage is essential *in vivo* (Chaudhuri *et al*, 2001; Paul *et al*, 2007).

The GroEL/GroES system has been the subject of extensive structural and functional analysis (reviewed in Hartl and Hayer-Hartl, 2002; Horwich *et al*, 2007). GroEL is an ~800 kDa cylindrical complex consisting of two stacked heptameric rings of ~57 kDa subunits. Each subunit of GroEL is composed of an equatorial ATPase domain, an apical domain and an intermediate hinge-like domain. The apical domains expose hydrophobic amino-acid residues towards the central cavity for the binding of non-native protein. GroES, a single heptameric ring of ~10 kDa subunits, caps the substrate-bound ring of GroEL. This step is dependent on ATP binding to the interacting GroEL ring (*cis*-ring) and results in the displacement of bound substrate into an enclosed cage generally large enough for proteins up to ~60 kDa. Importantly, upon binding of ATP and GroES, GroEL undergoes a dramatic conformational change resulting in an enlarged hydrophilic cavity with a net-negative charge of 42. Substrate protein is allowed to fold inside this cage for about 10 s, the time needed for the hydrolysis of the seven ATP bound in the GroEL *cis*-ring. Once hydrolysis is complete, ATP binding to the *trans*-ring causes the dissociation of GroES and release of the enclosed substrate. Incompletely folded protein is rapidly recaptured by an open GroEL ring for another folding attempt inside the cage. However, proteins that are too large to be encapsulated, such as yeast mitochondrial aconitase (82 kDa) and *E. coli* maltodextrin glucosidase (69 kDa), can nevertheless utilize GroEL for folding by cycling on the GroEL ring in *trans* to GroES (Chaudhuri *et al*, 2001; Paul *et al*, 2007). Indeed, several proteins larger than 60 kDa were found to interact with GroEL/GroES complexes (Kerner *et al*, 2005), suggesting that *trans*-folding may be used more widely (Horwich *et al*, 2007). Since *trans*-folding depends on the regulatory function by GroES, this mechanism could also explain the essential role of GroEL and GroES in cell physiology.

To determine whether folding by encapsulation is an essential element of chaperonin function *in vivo*, we tested a series of GroEL mutants with a reduced cavity size or altered cavity wall charge for their ability to functionally replace wild-type (WT)-GroEL. A stepwise reduction in cage size resulted in a gradual loss of cell viability. Mutant GroEL that was no longer able to encapsulate substrate failed to support cell growth, although protein binding and the ability to support *trans*-folding was preserved. Thus protein folding

*Corresponding author. FU Hartl or M Hayer-Hartl, Cellular Biochemistry, MPI of Biochemistry, Am Klopferspitz 18, Martinsried 82152, Germany. Tel.: +49 89 8578 2233; Fax: 49 89 8578 2211 or Tel.: +49 89 8578 2204; Fax: 49 89 8578 2211; E-mails: uhartl@biochem.mpg.de or mhartl@biochem.mpg.de

¹These authors contributed equally to this work

²Present address: Center for Cancer Research, Massachusetts Institute of Technology, Cambridge, MA 02139, USA

³Present address: Department of Biology, Massachusetts Institute of Technology, 77 Massachusetts Avenue, Cambridge, MA 02139, USA

Received: 3 January 2008; accepted: 27 March 2008; published online: 17 April 2008

by the encapsulation mechanism is an essential function of the chaperonin system.

Results

Reducing GroEL cavity size and net charge results in loss of *E. coli* viability

To test whether substrate enclosure in the chaperonin cage is essential for folding *in vivo*, we made use of a series of GroEL mutants with gradually reduced cavity size and encapsulation capacity (Tang *et al*, 2006). In these mutants, the flexible C-terminal [GGM]₄ repeat sequences (~1.3 kDa per GroEL subunit) that protrude from the equatorial GroEL domains into the central cavity are either deleted (EL-ΔC) or repeated up to four times (EL-2[GGM]₄ to EL-4[GGM]₄). This results in either the deletion of ~9 kDa or the addition of up to ~27 kDa mass per heptameric GroEL ring. The GroEL mutants were co-expressed with WT-GroES under IPTG control in an MC4100 *E. coli* strain, in which the chromosomal *groE* operon is under the tight control of the arabinose (P_{BAD}) promoter (Kerner *et al*, 2005). IPTG induction leads to two to threefold higher chaperonin levels than expression under the endogenous *groE* promoter. Growth of this strain in the absence of arabinose is only observed when functional GroEL/GroES is expressed (Figure 1). Expression of WT-GroEL alone in the absence of arabinose failed to support cell growth at 37°C, confirming that both GroEL and GroES are indispensable (Fayet *et al*, 1989). Mutants ELΔC and EL-2[GGM]₄, either lacking the disordered [GGM]₄ tails or having a tail duplication, complemented as efficiently as WT-GroEL/GroES (Figure 1). However, further reduction in cavity size resulted in a gradual loss of viability, with an estimated 10- and 1000-fold drop in cell numbers for mutants EL-3[GGM]₄ and EL-4[GGM]₄, respectively (Figure 1). This effect was also observed at growth temperatures of 30 and 42°C (data not shown).

Next, we tested the ability of GroEL mutants with a reduced negative net charge of the *cis*-cavity wall to function-

ally replace WT-GroEL. These mutants are impaired in the folding of specific model substrates *in vitro* but are active in folding other proteins; they are functional in substrate binding, GroES-mediated encapsulation and release (Tang *et al*, 2006). In EL-NNQ, the *cis*-cavity net charge of -42 of WT-GroEL is reduced to -21, due to the mutation of three negatively charged amino acids to neutral (D359N, D361N and E363Q) in each subunit of the heptameric GroEL rings. These changes did not impair the function of GroEL *in vivo* (Figure 1). However, EL-3N3Q, containing three additional negative-to-neutral mutations (E252Q, D253N, E255Q), failed to complement. Failure to support cell growth was also observed for EL-KKK2, in which three negatively charged amino acids are mutated to positive (D359K, D361K, E363K) (Figure 1). Both, EL-3N3Q and EL-KKK2 have a *cis*-cavity net charge of 0.

The failure of the GroEL mutants with reduced cavity size or net-charge to support *E. coli* growth may have resulted from their inability to either encapsulate essential cytosolic proteins or to provide a physical cavity environment conducive to their folding, respectively. Alternatively, some of the mutations may have affected the ability of GroEL to capture non-native substrate or may have changed the allosteric properties of the GroEL ATPase (Yifrach and Horovitz, 2000).

GroEL cavity mutants are functional in substrate binding

A series of experiments was conducted to explore the possible impact of the cavity mutations on the ability of GroEL to capture non-native proteins. We first tested the binding capacity of the GroEL cavity size-mutants in the absence of ATP in an *in vitro* aggregation prevention assay with mitochondrial rhodanese as a model substrate (Martin *et al*, 1991). This protein aggregates rapidly upon dilution from denaturant, as followed by an increase in absorbance at 320 nm (Figure 2A). Although GroEL suppressed aggregation completely, a 5–25% residual aggregation was noted for the

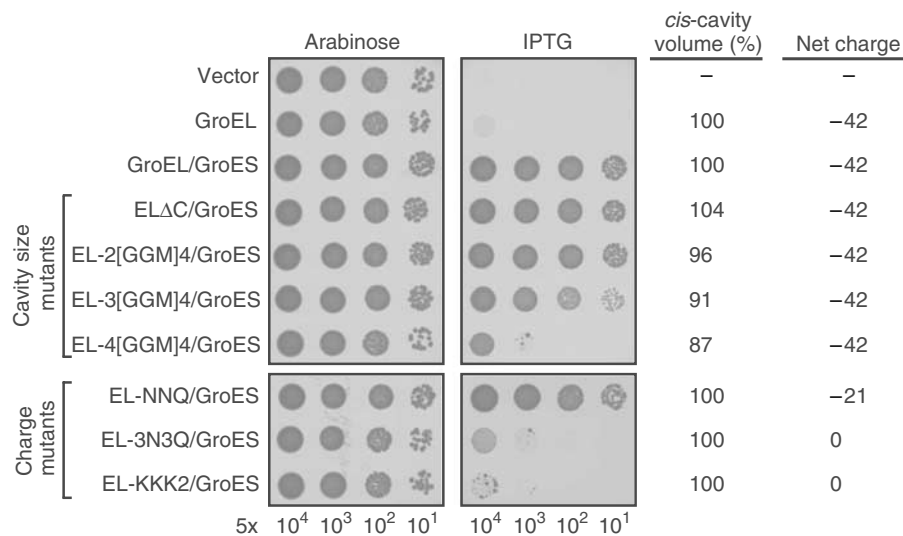


Figure 1 *In vivo* functionality of GroEL cavity-mutants. Constructs encoding the proteins indicated were transformed into *E. coli* MC4100 SC3 Kan^R cells. Cells were grown in the presence of arabinose for expression of WT-GroEL/GroES. Serial dilutions corresponding to cell numbers indicated were plated on arabinose-containing plates for continued expression of WT-GroEL/GroES or IPTG-containing plates for expression of GroEL-mutants/GroES at 37°C as described in Materials and methods.

cavity size-mutants scaling with the length of the C-terminal extensions (Figure 2A, left panel). Doubling the concentration of chaperonin relative to rhodanese resulted in nearly complete suppression of aggregation (Figure 2A, right panel). Fully efficient aggregation prevention was also observed for the cavity charge mutants (Supplementary Figure S1).

As prevention of aggregation provides only a semi-quantitative measure of GroEL substrate affinity, substrate binding was analysed directly by testing the ability of the GroEL mutants to form binary complexes with proteins varying in size, including rhodanese (33 kDa), and the authentic GroEL substrates METK (*S*-adenosyl methionine synthetase; 42 kDa) and SYT (threonyl-tRNA synthetase; 74 kDa) of *E. coli* (Kerner *et al*, 2005). Denatured proteins were diluted into buffer solution containing an equimolar concentration of either WT-GroEL, EL-2[GGM]₄ or EL-4[GGM]₄, followed by

size-exclusion chromatography. Efficient complex formation with mutant GroEL was observed with all substrates tested, whereas aggregated proteins formed in the absence of GroEL were not recovered from the sizing column (data not shown). The ability of EL-2[GGM]₄ to capture the unfolded proteins was reduced by 1–5% and that of EL-4[GGM]₄ by 9–25% relative to WT-GroEL (Figure 2B). The slightly earlier elution of substrate complexes with EL-4[GGM]₄, which was most pronounced with SYT (74 kDa), may suggest that the bound substrate protrudes from the smaller cavity more than in the case of WT-GroEL or EL-2[GGM]₄.

As an additional measure of substrate binding, we tested the capacity of the GroEL mutants to inhibit the spontaneous refolding of maltose-binding protein (MBP) upon dilution from denaturant. The GroEL and single-ring (SR)-EL cavity-size-mutants up to 3[GGM]₄ showed nearly WT efficiency in

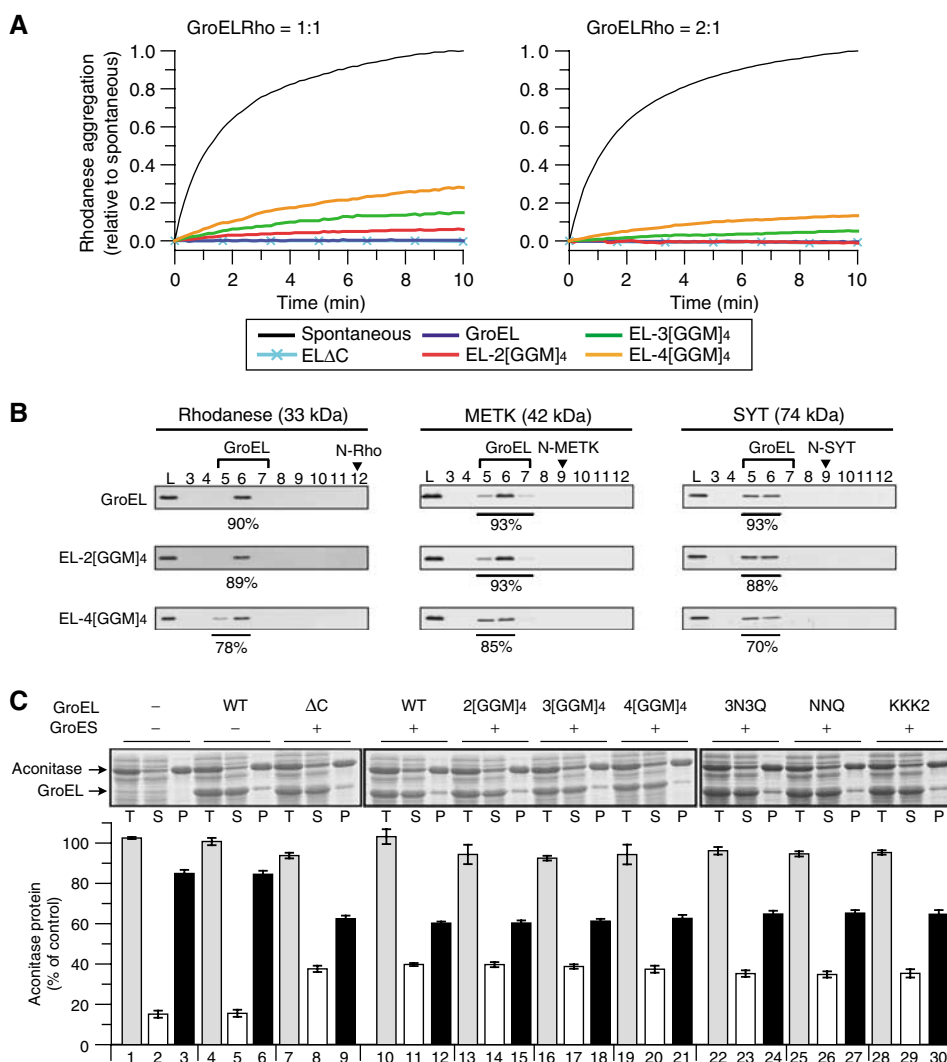


Figure 2 Substrate binding and *trans*-folding of GroEL cavity-mutants. **(A)** Prevention of rhodanese (Rho) aggregation *in vitro* was measured at an equimolar ratio of GroEL/rhodanese or at a twofold molar excess of GroEL (see Materials and methods). Aggregation after 10 min of rhodanese dilution from denaturant in the absence of chaperonin was set to 1. **(B)** Binary complexes of GroEL and GroEL-mutants with rhodanese, METK or SYT, produced by dilution of the denatured substrate proteins into GroEL-containing buffer, were analysed by size-exclusion chromatography. GroEL-bound substrates were quantified by immunoblotting with the loading control (L) set to 100%. Fractionation of GroEL and free native substrate proteins is indicated. **(C)** Capacity of GroEL cavity-mutants to support the soluble expression of the *trans*-folding substrate, yeast aconitase. Aconitase was overexpressed in *E. coli* BL21 cells with or without co-overexpression of WT-GroEL and GroEL-mutants with or without GroES at 37°C as indicated. Total (T), supernatant (S) and pellet (P) fractions of cells were analysed on SDS-PAGE and aconitase was quantified by densitometry. Standard deviations of at least three independent experiments are shown.

slowing MPB refolding, whereas the 4[GGM]₄ variants inhibited with slightly reduced efficiency (Supplementary Figure S2). In contrast, all the cavity size-mutants completely inhibited the refolding of a slow-folding double mutant of MBP, whose folding properties resemble those of authentic GroEL substrates (Supplementary Figure S3; Tang *et al*, 2006). In summary, based on a variety of assays, the substrate-binding efficiency of the 2[GGM]₄ variants is equivalent to WT-GroEL and that of the 3[GGM]₄ and 4[GGM]₄ variants is reduced by ~10 and ~25%, respectively. These results differ from recent findings by Farr *et al* (2007), who reported a 70–90% reduction in the binding efficiency for a GroEL mutant with 4[GGM]₄ tails.

To assess the functionality of the GroEL cavity-mutants in substrate binding and GroES cycling *in vivo*, we analysed their ability to support protein folding without encapsulation by the so-called *trans*-mechanism. In this mechanism, substrates such as yeast aconitase (82 kDa) fold by cycling on the GroEL ring in *trans* to GroES (Chaudhuri *et al*, 2001). Upon expression of yeast aconitase in *E. coli*, only ~17% of the protein was recovered in the soluble fraction (Figure 2C, lanes 1–3). Whereas co-expression of WT-GroEL alone did not improve the folding yield, co-expression of both GroEL and GroES increased the yield of soluble aconitase to ~39% (Figure 2C, lanes 4–6 and 10–12), consistent with the GroES dependence of *trans*-folding (Chaudhuri *et al*, 2001). The GroEL cavity size- and charge-mutants all enhanced the yield of soluble aconitase to the same extent (Figure 2C, lanes 7–30), confirming that they are functional in substrate binding and ATP-dependent GroES cycling *in vivo*.

The results from the *in vitro* binding analyses and the functional *in vivo* assays demonstrate that the GroEL cavity-mutants preserve the ability to bind and release non-native proteins. Thus, the failure of the size-mutant, EL-4[GGM]₄, and the charge-mutants, EL-3N3Q and EL-KKK2, to replace WT-GroEL *in vivo* is probably due to their impaired ability to mediate folding of essential proteins by the encapsulation mechanism (Figure 1).

GroEL size-mutants have a reduced capacity to encapsulate substrates *in vivo*

Most *E. coli* proteins that interact with GroEL for folding are smaller than 60 kDa in size and thus could be enclosed in the chaperonin cage (Kerner *et al*, 2005). To test whether reducing the cavity volume limits the size range of substrates that can be encapsulated *in vivo*, we applied an established pull-down assay to isolate mutant-GroEL/GroES complexes with enclosed substrate from cell extracts. A His₆-tagged version of GroES from *Methanosarcina mazei* (*Mm*) was transiently co-expressed with the GroEL size-mutants in *E. coli* MC4100 cells, expressing endogenous GroEL/GroES. *Mm*GroES is fully functional in *E. coli* but results in a more stable interaction with GroEL, facilitating the isolation of complexes upon rapid conversion of ATP to ADP by glucose/hexokinase during cell lysis (Kerner *et al*, 2005). Substrate proteins up to ~60 kDa are enclosed in the isolated GroEL/*Mm*GroES complexes (Figure 3A), protected against externally added protease (Kerner *et al*, 2005).

No chaperonin complexes were isolated in the absence of His₆-*Mm*GroES expression (Figure 3B, lane 1). The GroEL mutants bound *Mm*GroES with an efficiency similar to WT-GroEL, as revealed by immunoblotting of pull-down reactions

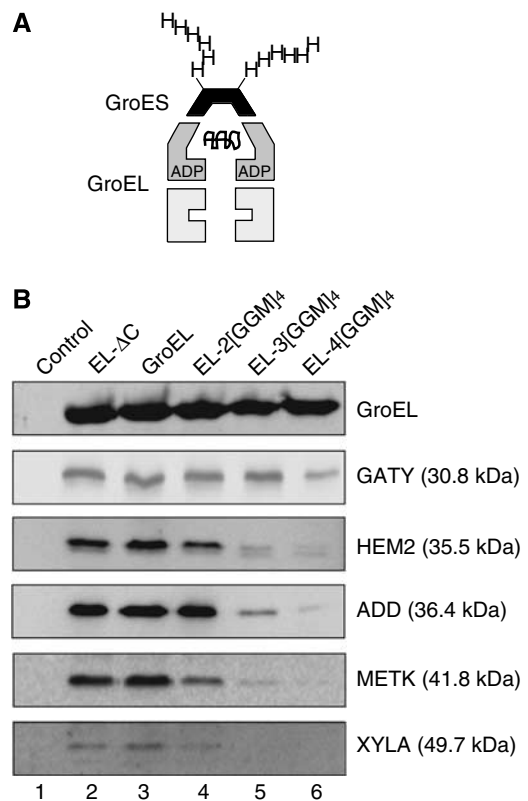


Figure 3 Encapsulation efficiency of endogenous substrates by GroEL cavity size-mutants. (A) Schematic representation of complexes of GroEL with His₆-tagged *Mm*GroES arrested in the ADP state with substrate enclosed within the *cis*-cavity. (B) *E. coli* MC4100 cells overexpressing GroEL cavity size-mutants and His₆-tagged *Mm*GroES were lysed, and chaperonin complexes containing endogenous substrates were isolated as described in Materials and methods. The substrate proteins indicated were detected by immunoblotting. GroEL was detected with the anti-serum against XYLA, which has strong GroEL cross-reactivity. To control for specificity, the same isolation procedure was performed with cells overexpressing WT-GroEL and non-His₆-tagged *Mm*GroES.

(Figure 3B, top panel). As shown by immunoblotting against specific substrates, WT-GroEL and ELΔC permitted the efficient encapsulation of proteins ranging from 31 to 50 kDa (Figure 3B, lanes 2 and 3). EL-2[GGM]₄ showed a substantially reduced encapsulation for METK (~42 kDa) and XYLA (~50 kDa) (Figure 3B, lane 4). EL-3[GGM]₄ was still able to enclose the ~31 kDa protein, GATY, but displayed a strongly reduced encapsulation efficiency for the larger substrates (Figure 3B, lane 5). EL-4[GGM]₄ showed a partial reduction in encapsulation already with the smallest substrate (~31 kDa) and essentially complete loss of encapsulation with the larger proteins (Figure 3B, lane 6). As the cavity size-mutants efficiently bind unfolded protein and form stable substrate/GroEL complexes (Figure 2 and Supplementary Figures S2 and S3), we conclude that the stepwise reduction in cavity size is responsible for the gradual loss in substrate encapsulation by GroES, thus explaining the reduced function of EL-3[GGM]₄ and the loss of function of EL-4[GGM]₄ *in vivo* (Figure 1).

Enhanced folding of GFP in a smaller GroEL cavity

Reducing the size of the GroEL/GroES cage may accelerate the folding of relatively small proteins (~30 kDa), due to

steric confinement of folding intermediates (Hayer-Hartl and Minton, 2006; Tang *et al*, 2006). If the chaperonin cavity has a critical role in folding, this effect may also lead to an increase in folding yield *in vivo*. To test this possibility, we chose WT green fluorescent protein (GFP; 27 kDa) as an aggregation-prone model substrate (Wang *et al*, 2002). Overexpression of WT-GroEL and GroES at 30°C enhanced the solubility of GFP from 10 to 40% (Figure 4A, lanes 2 and 8) and increased GFP fluorescence sevenfold (Figure 4B), consistent with previous findings (Wang *et al*, 2002). Strikingly, co-overexpression with EL-2[GGM]₄/GroES, which has a moderately reduced cavity size, improved the solubility of GFP to 60% (Figure 4A, lane 11) and increased GFP fluorescence more than tenfold (Figure 4B). On the other hand, EL-3[GGM]₄ was less efficient than WT-GroEL, and EL-4[GGM]₄ was inactive in supporting GFP folding (Figure 4A and B). Deleting the C-terminal tails in EL-ΔC also markedly reduced folding yield (Figure 4A, lane 5 and Figure 4B).

Refolding experiments *in vitro*, monitoring the gain in GFP fluorescence, were performed to investigate this effect in more detail. As GFP refolding is biphasic (Fukuda *et al*, 2000; Iwai *et al*, 2001), apparent folding rates are presented as the weighted average of fast and slow phases ($\sim 27 \times 10^{-3}$ and $\sim 5 \times 10^{-3} \text{ s}^{-1}$, respectively), based on their relative amplitudes. Spontaneous refolding of denatured GFP resulted in the recovery of $\sim 35\%$ native protein (Figure 4C), as refolding was limited by aggregation. WT-GroEL/GroES and ATP increased the yield by $\sim 50\%$ and accelerated folding approximately twofold (Figure 4C and D). The improved

yield was predominately due to an increase in the amplitude of the fast-folding phase. A substantial further increase in yield and a moderate rate enhancement was observed with EL-2[GGM]₄, whereas folding efficiency was markedly reduced with EL-3[GGM]₄ and EL-4[GGM]₄ (Figure 4C and D). As shown below, accelerated folding was more pronounced with the SR-EL variant of 2[GGM]₄ (Figure 6B). In contrast to the observations *in vivo* (Figure 4A and B), refolding with ELΔC *in vitro* was similarly efficient as WT-GroEL (Figure 4C and D). This discrepancy may be due to the coupling of folding and fluorophore formation *in vivo*, whereas the protein used for the *in vitro* experiments has a preformed fluorophore. These results demonstrate that the mutations changing the size of the GroEL cavity affect both the yield and rate of GFP folding. A moderate reduction in cavity size appears to be optimal for the folding of GFP, whereas further reduction is inhibitory, presumably restricting rearrangement necessary for folding.

Restriction of substrate motility in GroEL mutants with reduced cavity size

Steady-state fluorescence anisotropy measurements with GFP (27 kDa) and a fusion protein of mouse dihydrofolate reductase and GFP (DHFR-GFP, ~ 50 kDa) were performed to evaluate the effect of steric confinement by the chaperonin cage. GroES-mediated encapsulation of the proteins was performed in non-cycling single-ring (SR) versions of WT-GroEL and cavity size-mutants. SR-EL is functionally similar to WT-GroEL, but undergoes only one round of ATP

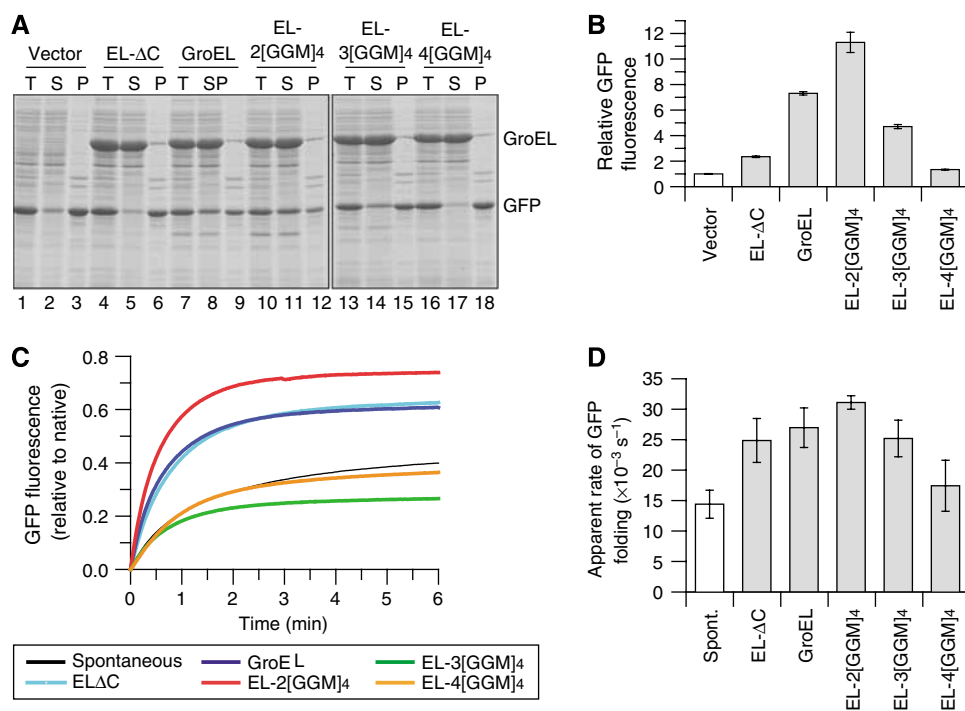


Figure 4 Enhanced folding of GFP upon mild reduction of GroEL cavity size. Solubility (A) and fluorescence (B) of WT-GFP upon co-overexpression with GroEL cavity size-mutants and GroES in *E. coli* MC4100 cells at 30°C. Cells were grown and analysed as in Figure 2C (see Materials and methods). Total (T), supernatant (S) and pellet (P) fractions from equal amounts of cells were analysed by SDS-PAGE and Coomassie staining. GFP fluorescence was measured in cell lysates containing equal amounts of total protein with the activity in the vector only control set to 1. Standard deviations of at least three independent experiments are shown. (C) and (D) Kinetics and yield of GFP refolding with GroEL cavity size-mutants and GroES *in vitro*. Refolding yields are plotted with the native GFP control set to 1. Refolding traces were fitted to a double exponential equation and apparent rates are plotted as the weighted average of the slow and fast rates based on their relative amplitudes. Standard deviations of at least three independent experiments are shown.

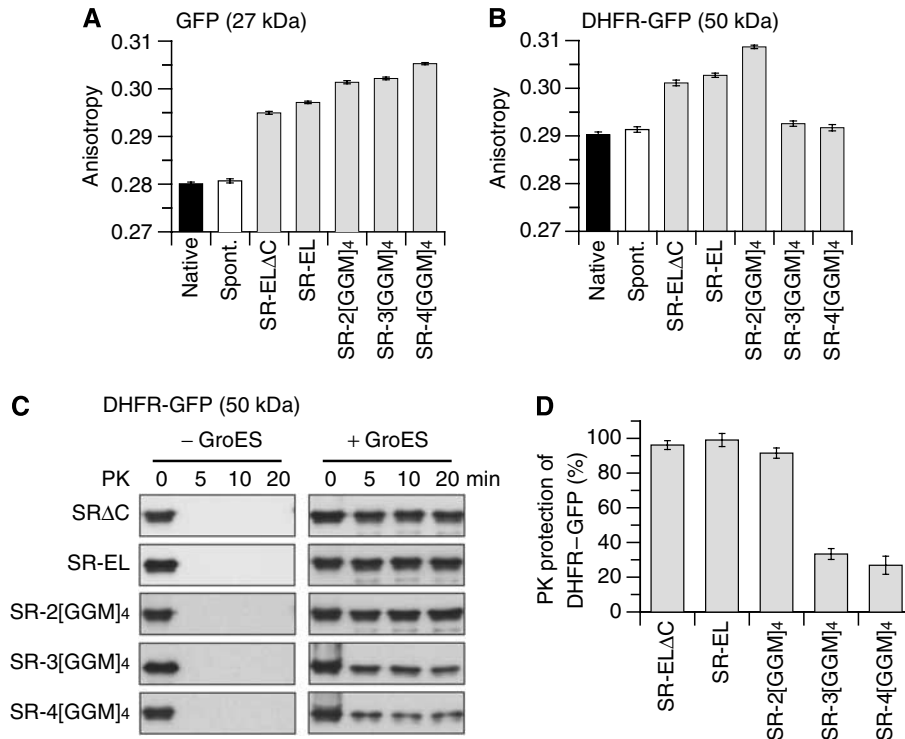


Figure 5 Motility and protease protection of substrate protein upon encapsulation in SR-EL cavity size-mutants. Steady-state fluorescence anisotropy of GFP (**A**) and DHFR-GFP fusion protein (**B**) upon addition of GroES and AMP-PNP to binary SR-EL-substrate complexes. Anisotropy values of native and spontaneously refolded proteins are shown as controls (see Materials and methods). Standard deviations of at least three independent experiments are shown. (**C**) and (**D**) Protease protection of DHFR-GFP upon addition of GroES and AMP-PNP to binary SR-EL-substrate complexes. Proteinase K (PK) protected DHFR-GFP was detected by immunoblotting with anti-GFP antibody and quantified by densitometry. Standard deviations of three independent experiments are shown.

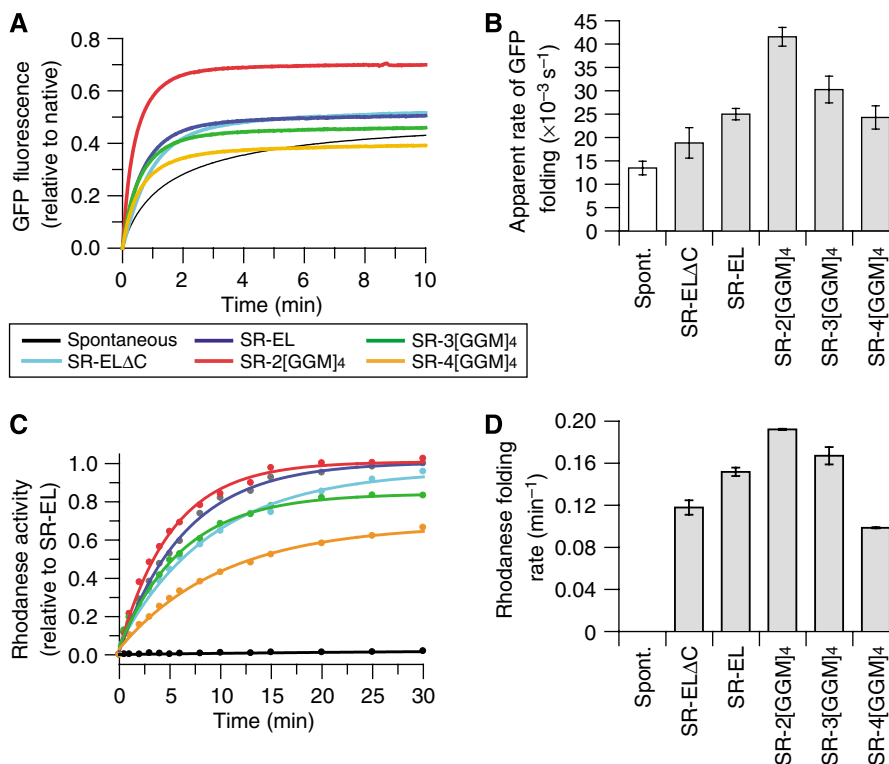


Figure 6 Accelerated folding of GFP and rhodanese in cavity size-mutants is independent of ongoing ATP-hydrolysis. Kinetics and yield of WT-GFP refolding (**A**, **B**) and of rhodanese refolding (**C**, **D**) with SR-EL cavity size-mutants and GroES/ATP *in vitro*. Refolding yields are plotted with the native GFP and rhodanese control set to 1, respectively. Refolding traces for GFP were fitted as in Figure 4D and refolding traces for rhodanese were fitted to a single exponential equation. Note that there is essentially no spontaneous renaturation of rhodanese under the experimental conditions. Standard deviations of at least three independent experiments are shown.

hydrolysis, forming a stable complex with GroES and encapsulated substrate (Weissman *et al*, 1996). Substantially higher anisotropy values were obtained for GFP upon enclosure in the stable *cis*-cavity than for the free native or spontaneously refolded protein (Figure 5A), reflecting the reduced mobility of the molecule inside the chaperonin cage. Enclosure in SR-2[GGM]₄, SR-3[GGM]₄ and SR-4[GGM]₄ resulted in a gradual increase in GFP anisotropy, indicating that the stepwise extension of the C-terminal GroEL sequences results in an increased steric confinement of the enclosed protein (Figure 5A). Encapsulation in SR-2[GGM]₄ also caused an increase in anisotropy for the larger protein DHFR-GFP, but the anisotropy values observed with SR-3[GGM]₄ and SR-4[GGM]₄ were as low as those of free DHFR-GFP (Figure 5B). This suggests that GroES-mediated encapsulation of DHFR-GFP in SR-3[GGM]₄ and SR-4[GGM]₄ is no longer possible and that the protein is instead displaced from the chaperonin complex.

To address this possibility, we tested the accessibility of DHFR-GFP to proteinase K (PK), based on previous observations that substrate protein encapsulated in SR-EL by GroES is protease protected (Hayer-Hartl *et al*, 1996; Weissman *et al*, 1996). Non-native DHFR-GFP bound to chaperonin in the absence of GroES was readily degraded, whereas encapsulation in SR-ΔC, SR-EL and SR-2[GGM]₄ resulted in complete protease protection (Figure 5C and D). In contrast, when bound to SR-3[GGM]₄ or SR-4[GGM]₄, addition of GroES resulted in only 25–30% protease protection (Figure 5C and D), indicating that stable encapsulation no longer occurred. The residual protease resistance may be due to the folding or misfolding of some DHFR-GFP upon its displacement from chaperonin.

Together, these results provide direct evidence that reducing cavity size effectively restricts the motility of the enclosed 27 kDa GFP. Whereas a mild reduction in cavity volume in the EL-2[GGM]₄ variant is associated with enhanced GFP folding (Figure 4), the more marked volume reduction in EL-3[GGM]₄ results in the exclusion of substrate proteins of ~35 kDa and greater (Figures 3 and 5).

Relationship of folding rate and GroEL ATPase activity

The chaperonin cycle is allosterically regulated by ATP binding and hydrolysis (Yifrach and Horovitz, 2000). GroES binds and unbinds from GroEL approximately every 10–15 s, the time needed for completion of ATP-hydrolysis in the GroEL *cis*-ring. GroES dissociation results in the release of enclosed substrate, with incompletely folded protein rapidly rebinding to an open GroEL ring. Many substrates interact with GroEL for several reaction cycles and it has been suggested that rebinding serves to repeatedly unfold kinetically trapped intermediates, thereby allowing faster folding speeds ('iterative annealing') (Thirumalai and Lorimer, 2001). To test whether the acceleration of folding of ~30 kDa proteins observed upon reducing GroEL cavity size is dependent on GroES cycling, we performed *in vitro* refolding experiments with SR-EL size-mutants, in which folding occurs upon a single round of encapsulation (Weissman *et al*, 1996). Importantly, the rate acceleration of GFP folding observed with the cycling GroEL system (Figure 4C and D) was reproduced with the non-cycling SR-EL size-mutants (Figure 6A and B). Again, optimal folding rate and yield was obtained with the 2[GGM]₄ size-mutant. Similarly, a folding rate

acceleration of rhodanese (33 kDa) was observed with SR-EL-2[GGM]₄/GroES (Figure 6C and D). As under the experimental conditions, the SR-2[GGM]₄/GroES complex encapsulates substrate stably (Figure 5C and D), the ability of this cavity size-mutant to enhance the folding kinetics of GFP and rhodanese is independent of iterative GroEL ATPase cycles. The use of SR-EL in these experiments also rules out possible effects of substrate or residual denaturant on the steady-state GroEL ATPase as the cause of accelerated folding.

It has also been suggested that an increase of the GroEL ATPase activity could contribute to the effects on folding rate observed with the GroEL size-mutants by altering the dwell time of substrate in the *cis*-cavity (Farr *et al*, 2007). ATPase measurements showed that extension of the C-terminal GroEL sequences results in a two- to threefold increase of the maximal GroEL ATPase activity, dependent on assay conditions (Figure 7A and Supplementary Figure S4). However, the ATPase activity did not increase linearly with the length of the C-terminal extensions, as reported by Farr *et al* (2007), but rather reached a plateau with the 2[GGM]₄ mutant. Importantly, the ability of GroES to inhibit the ATPase activity by ~50% was preserved. The dependence of ATPase activity on ATP concentration was similar for WT-GroEL and GroEL tail extension-mutants, with half-maximal rates being observed at 6–12 μM ATP (Supplementary Figure S4). As the tail extension-mutants have similar ATPase activities, the decrease in folding rate and yield observed with EL-3[GGM]₄ and EL-4[GGM]₄ relative to EL-2[GGM]₄ (Figure 4) is unrelated to the ATPase activation but is rather a consequence of the reduction of *cis*-cavity size. Although, in the case of EL-2[GGM]₄, the enhanced ATPase may have increased substrate turnover and thus the yield of GFP refolding *in vivo* (Figure 4A and B) (Tehver and Thirumalai, 2008), it is likely that the reduced cavity size contributed to this effect. This is supported by our observation with SR-2[GGM]₄ in which folding rate is independent of ongoing ATP hydrolysis (Figure 6).

To test whether the activation of the GroEL ATPase affects the folding rate upon a single round of encapsulation, we generated GroEL cavity size-mutants containing the additional mutation D398A in the ATPase domain. GroEL(D398A) binds ATP and GroES but hydrolyzes ATP extremely slowly (Rye *et al*, 1997). As a result, substrate encapsulation and folding occurs upon single-round encapsulation as in SR-EL, but with very slow ATP-hydrolysis. As expected, GroEL(D398A), EL-2[GGM]₄(D398A) and EL-3[GGM]₄(D398A) had negligible ATP-hydrolysis rates of ~2% of WT-GroEL (Figure 7B). The rate and yield of GFP folding with GroEL(D398A) was reduced by ~25% compared with WT-GroEL. Importantly, EL-2[GGM]₄(D398A) resulted in an ~50% increase in folding rate and yield relative to GroEL(D398A). This effect was reversed with EL-3[GGM]₄(D398A) (Figure 7C), reproducing the results observed with the GroEL and SR-EL tail extension-mutants (Figures 4D and 6B). Similar results were obtained with rhodanese. Again folding was accelerated with EL-2[GGM]₄(D398A) and slowed with EL-3[GGM]₄(D398A) (Figure 7D).

These experiments failed to demonstrate a dependence of folding rate on the GroEL ATPase over a range of ATPase activities from close to 0 to ~3-fold higher than WT, both in the cycling and non-cycling systems. This is consistent with a

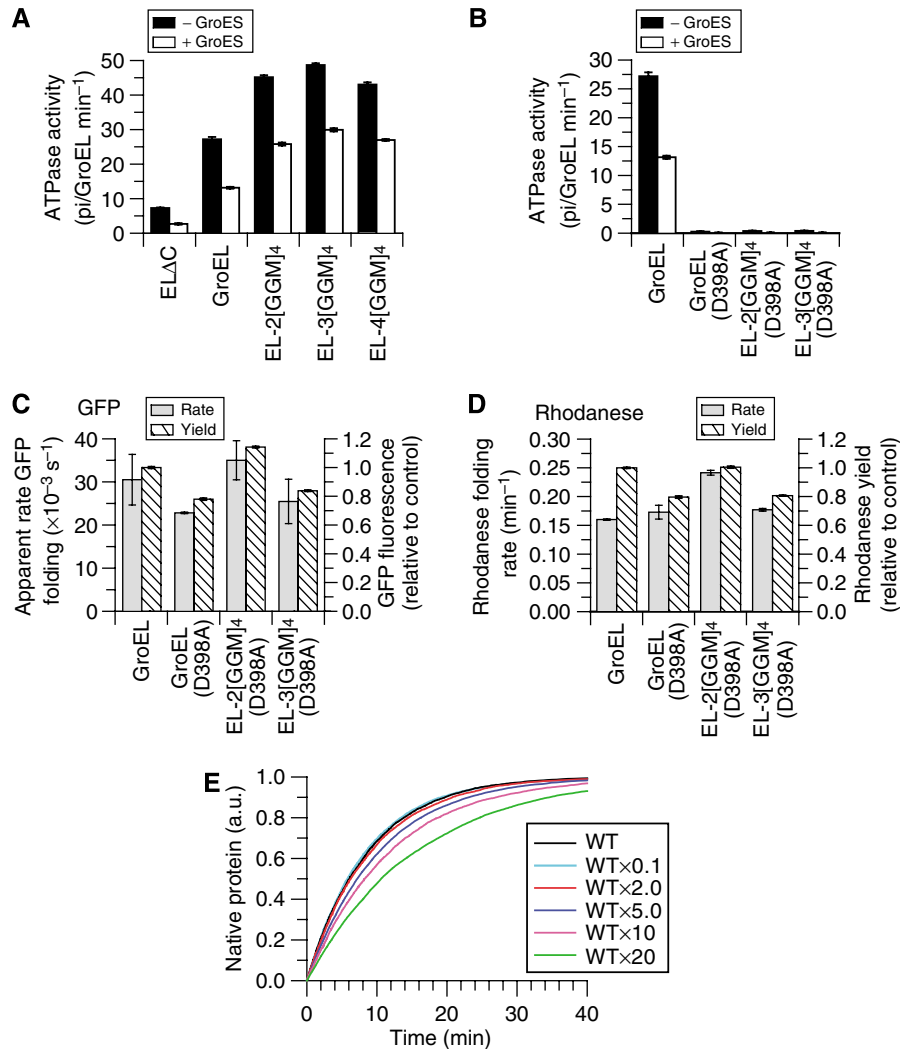


Figure 7 Accelerated folding by GroEL cavity size-mutants is independent of the rate of ATP hydrolysis. Steady-state ATPase activities of GroEL cavity size-mutants (**A**) and ATPase-deficient GroEL(D398A) cavity size-mutants (**B**) at 25°C. ATPase rates are indicated in ATP hydrolyzed per GroEL tetradecamer per min (see Materials and methods). Refolding yields and rates of WT-GFP (**C**) and rhodanese (**D**) with GroEL(D398A) cavity size-mutants and GroES/ATP. Refolding traces for GFP were fitted as in Figure 4D and refolding traces for rhodanese were fitted to a single exponential equation. The refolding yield obtained with WT-GroEL/GroES was set to 1. Standard deviations of at least three independent experiments are shown. (**E**) Simulation of rhodanese folding kinetics dependent on GroEL/GroES cycling rate at excess chaperonin over substrate. The binding rate of unfolded protein to GroEL was set to $2 \times 10^7 \text{ M}^{-1} \text{ s}^{-1}$ (Rye *et al*, 1999) and binding of GroES to GroEL-substrate complexes was set to $1 \times 10^6 \text{ M}^{-1} \text{ s}^{-1}$ (KC and SS, unpublished data, 2007). The rate of rhodanese refolding with WT-GroEL/GroES or SR-EL/GroES was set to $2.5 \times 10^{-3} \text{ s}^{-1}$ (Figure 7D). The normal ATPase-induced cycling rate was fixed at 0.07 s^{-1} with an approximate half-time of 10 s. The simulation was performed using chemical kinetics simulator (CKS) (http://www.almaden.ibm.com/st/computational_science/ck). The ATPase-induced cycling rate was varied between 0.1- and 20-fold of the normal rate and refolding rates are plotted. The concentrations used for the simulation were GroEL 1 μM , GroES 2 μM and rhodanese 0.5 μM (see Supplementary Figure S5 for a kinetic model for the simulation).

theoretical simulation of rhodanese folding during GroEL/GroES cycling. In this simulation, GroEL is in excess over protein substrate, such that essentially all non-native protein is GroEL associated. Folding is assumed to occur only upon protein encapsulation in the GroEL/GroES cage, at a rate equivalent to spontaneous folding (Brinker *et al*, 2001). A two- to fivefold increase in steady-state ATPase is predicted to have little effect on folding rate, whereas a further rate increase begins to slow folding due to the reduction of the dwell time of rhodanese in the *cis*-cavity and a corresponding increase of the dwell time in the GroEL-bound state (Figure 7E and Supplementary Figure S5). Reducing the ATPase activity has no effect on folding rate, consistent with the finding that a single round of encapsulation by SR-EL results in fully efficient folding.

Discussion

Essential role of GroEL/GroES as a folding compartment

The GroEL/GroES chaperonin system functions as a protein folding cage based on experiments *in vitro* (Mayhew *et al*, 1996; Weissman *et al*, 1996), but whether folding by encapsulation underlies the essentiality of GroEL and GroES for *E. coli* growth (Fayet *et al*, 1989) had remained unclear. To determine whether the chaperonin cavity is dispensable for *E. coli* growth, we tested the *in vivo* functionality of GroEL mutants displaying modified cavity properties. GroEL versions with a reduced cavity size, precluding efficient encapsulation of substrates greater than $\sim 30 \text{ kDa}$, were no longer able to support *E. coli* growth. Likewise, removal of the net

negative charge of the *cis*-cavity wall resulted in loss of GroEL function. Importantly, these mutants preserved the ability to bind and release non-native substrate protein and GroES. The 10–25% reduction in substrate-binding capacity of GroEL-3[GGM]₄ and 4[GGM]₄ cannot account for the failure of these variants to support normal growth when considering that *E. coli* tolerates an ~90% reduction in GroEL levels without significant growth impairment (McLennan *et al*, 1993; Kerner *et al*, 2005). Thus, our findings demonstrate the essential role of the chaperonin compartment in protein folding *in vivo*. The GroEL/GroES folding cage probably provides its essential function by preventing protein aggregation during folding and by reducing kinetic folding barriers encountered by a subset of substrates.

Significance of GroEL cavity size and charge

The volume capacity of the GroEL/GroES cage is generally sufficient for proteins up to ~60 kDa. A special case is the encapsulation of an ~86 kDa assembly intermediate of the heterodimeric mitochondrial branched-chain α -ketoacid dehydrogenase, consisting of ~50.7 and ~35.5 kDa subunits (Chen *et al*, 2006). On the other hand, single protein molecules of ~69 and ~74 kDa cannot be encapsulated (Kerner *et al*, 2005; Paul *et al*, 2007). An additional mass of ~18 kDa per GroEL ring generated by triplicating the C-terminal [GGM]₄ repeat sequences in mutant EL-3[GGM]₄ resulted in a 10-fold drop in cell number in the absence of WT-GroEL. EL-4[GGM]₄, having an added mass of ~27 kDa per GroEL ring, was essentially unable to support *E. coli* growth (~1000-fold drop in cell number upon loss of WT-GroEL). Analysis of isolated chaperonin complexes showed that EL-3[GGM]₄ partially or completely excludes proteins greater than ~35 kDa and EL-4[GGM]₄ proteins greater than ~30 kDa. Consistent with these findings, the majority of GroEL-dependent *E. coli* proteins are between ~20 and 50 kDa, with six of the 13 substrates predicted to have essential function exceeding ~31 kDa in size (Kerner *et al*, 2005). Thus, the failure of EL-4[GGM]₄ to support *E. coli* growth can be explained by the exclusion of these essential proteins from the GroEL/GroES cage, resulting in their misfolding. The capacity of EL-2[GGM]₄ to replace WT-GroEL is consistent with the ability of this mutant to encapsulate proteins up to at least ~40 kDa (Tang *et al*, 2006 and this study); this would include all essential *E. coli* proteins predicted to be GroEL dependent, with the exception of D-amino acid dehydrogenase (~48 kDa) and topoisomerase IV (PARC, ~84 kDa) (Kerner *et al*, 2005). Notably, PARC is too large to be encapsulated even by WT-GroEL and may follow the *trans*-folding mechanism described for yeast aconitase (Chaudhuri *et al*, 2001).

As demonstrated with EL-2[GGM]₄, moderately restricting cavity space can accelerate the folding of proteins of ~30 kDa, such as GFP, resulting in substantially higher folding yields *in vivo*. Various mechanistic components may contribute to enhancing folding speed, including an effect of steric confinement, which would entropically destabilize the unfolded state and favor the formation of compact folded protein (Baumketner *et al*, 2003; Takagi *et al*, 2003). Anisotropy measurements provided direct evidence that multiplication of the C-terminal GroEL sequences restricts the motility of substrate protein upon encapsulation. For proteins of ~30 kDa (GFP and rhodanese), encapsulation in EL-2[GGM]₄ results in productive confinement, whereas

restricting motility further is inhibitory, presumably by hindering necessary rearrangement steps.

Independent evidence for the essential role of the chaperonin folding compartment was provided by our analysis of GroEL mutants with altered charge properties of the cavity wall. The inner surface of the GroEL ring exposes numerous positively and negatively charged amino-acid residues with a marked net negative charge of 42 (minus 6 per GroEL subunit). Many of the negatively charged residues are highly conserved among GroEL homologues (Brocchieri and Karlin, 2000). Whereas GroEL mutant EL-NNQ, having a reduced net charge of minus 21, fully supported *E. coli* growth, the complete removal of the negative net charge in EL-3N3Q or EL-KKK2 resulted in the loss of *in vivo* functionality. In contrast, these GroEL charge-mutants were unaffected in their ability to support the soluble expression of the *trans*-folding substrate aconitase. These results suggest that the negative charge property of the cavity is critical in the folding of some essential proteins by the encapsulation mechanism. The majority of GroEL-dependent *E. coli* proteins, including eight essential proteins, are negatively charged (pI values of 5.1–6.2) (Kerner *et al*, 2005) and thus could experience a repulsive force from the cavity wall that may facilitate folding. Such an effect may benefit many GroEL substrates, but it has also been shown that changing a single cavity-exposed aromatic residue on GroES to arginine (Y71R) can significantly improve the folding of a specific protein, GFP (Wang *et al*, 2002). This finding, together with our present results, suggests that a mutual adaptation of the physical properties of the chaperonin cavity and the natural GroEL substrate complement has occurred during evolution.

Folding rate acceleration and ATPase turnover

There are currently two models for acceleration of folding by the GroEL/GroES system. Although mechanistically distinct, these two models are not mutually exclusive. The central element of the 'iterative annealing' hypothesis suggests that the GroES-mediated movement of the apical GroEL domains exerts a stretching force on bound substrate protein, thereby actively unfolding kinetically trapped, misfolded intermediates (Thirumalai and Lorimer, 2001). This effect, occurring in every chaperonin ATPase cycle, would speed up folding by reducing the half-life of slow folding species and allowing their repartitioning with kinetically more effective folding routes. In contrast, 'cage-mediated annealing' (Tang *et al*, 2006) posits that the physical environment of the chaperonin cavity is critical in enhancing folding speed. To distinguish between these two models, we explored the dependence of folding rate on GroEL ATPase activity for GFP and rhodanese. Specifically, we tested the premise of the iterative annealing model that a faster ATPase rate, as observed in the GroEL size-mutants, would speed up folding by increasing the number of potential unfolding events. Contrary to this assumption, we found that the folding rates achieved with the cycling GroEL/GroES and the non-cycling SR-EL/GroES systems are identical within experimental error. Importantly, the rate enhancement of folding achieved by reducing the size of the *cis*-cavity is also observed with SR-EL/GroES and is thus independent of the ATPase acceleration.

In the presence of GroES, SR-EL carries out a single round of ATP-hydrolysis and then becomes arrested in the ADP state (Weissman *et al*, 1996). To test whether the rate of this

ATPase reaction may be critical for folding speed, we performed experiments with the D398A mutant of GroEL, which binds ATP normally but hydrolyzes it extremely slowly. Importantly, the accelerating effect of the tail extension-mutants on folding was preserved in GroEL(D398A), establishing that the effect of geometric confinement on folding speed is independent of ATP-hydrolysis by GroEL and only requires ATP-dependent GroES binding. Based on these results, it would appear that the main role of the GroEL ATPase is to drive the conformational transition of GroEL from the substrate binding-active to the folding-active state, allowing for folded protein to be discharged in a timely fashion.

As in a normal ATPase cycle the substrate protein spends only ~1 s or less in the folding-inactive GroEL-bound state and the vast majority of the cycle time (10–15 s) encapsulated within the folding-active *cis*-cavity, moderately increasing the GroEL ATPase would have little effect on folding rate. A simulation of the effect of ATPase rate on the folding speed of rhodanese supported this conclusion (Figure 7E and Supplementary Figure S5). Whereas a two- to fivefold increase in cycling rate was predicted to slow folding by only a small extent, a 10- to 20-fold increase would reduce the dwell time of the substrate in the *cis*-cavity more substantially and approximately double the half-time of folding for a protein like rhodanese. In contrast, decelerating the ATPase rate was shown to have virtually no effect on folding rate as long as GroEL is in excess over substrate, consistent with the observation that SR-EL/GroES allows folding at essentially the same rate as WT-GroEL/GroES. However, under conditions of substrate excess *in vivo*, both decelerating or accelerating the GroEL ATPase rate may reduce the folding yield for aggregation-sensitive substrates (Jewett and Shea, 2008; Tehver and Thirumalai, 2008). Prolonging the dwell time of substrate inside the cage would reduce the capacity of chaperonin to fold multiple substrate molecules, whereas reducing the dwell time may prevent completion of folding inside the cage and thus lead to the release of aggregation-prone intermediates.

Materials and methods

Strains and plasmids

GroEL mutants were constructed in a pCH vector backbone and purified as specified earlier (Chang *et al*, 2005; Tang *et al*, 2006). The GroEL ATPase-deficient mutants, EL-D398A, EL-2[GGM]₄-D398A and EL-3[GGM]₄-D398A, were generated by site-directed mutagenesis. Chaperonin constructs for *in vivo* co-expression were prepared by inserting mutated *groEL* DNA fragments from pCH-GroEL into the pOFXtac-SL2 vector (Castanié *et al*, 1997). The DHFR-GFP fusion construct was cloned by introducing a mouse DHFR PCR fragment into the pCH-L16-GFP vector encoding a C-terminal His₆-tag (Chang *et al*, 2005). WT GFP and yeast aconitase (a kind gift from S Rospert) were generated by subcloning the respective open reading frames into the arabinose promoter-controlled vector pBAD18 (Guzman *et al*, 1995).

Proteins

Chaperone proteins METK and SYT were purified as described previously (Hayer-Hartl *et al*, 1996; Kerner *et al*, 2005). WT GFP and DHFR-GFP were purified using a Ni-NTA column (Qiagen). Bovine mitochondrial rhodanese was from Sigma. Polyclonal antibodies against GroEL substrates were produced in rabbits.

In vivo complementation assay

A GroEL depletion strain, MC4100 SC3 *Kan*^R, in which the chromosomal *groE* promoter was replaced with the *araC* gene and

the pBAD promoter, was used (Kerner *et al*, 2005). *E. coli* MC4100 SC3 cells harbouring pOFXtac-SL2 plasmids for expression of GroEL/GroES or GroEL-mutants/GroES were grown in LB/0.05% arabinose medium at 30°C to OD₆₀₀ = ~1 (~7 h), when cell numbers were determined to be similar among all strains tested (~5 × 10⁸ cells ml⁻¹). Serial dilutions of cell suspension were spotted onto LB-spectinomycin selection plates containing 0.05% arabinose (for expression of WT-GroEL/GroES) or 0.1 mM IPTG (for expression of GroEL-mutants/GroES). Plates were incubated for ~16 h at 30, 37 or 42°C.

Rhodanese aggregation prevention assay

Rhodanese (50 μM) was denatured for 1 h at 25°C in denaturation buffer (6 M GuHCl, 20 mM Tris-HCl, pH 7.5, 20 mM KCl, 5 mM MgCl₂, 5 mM DTT) and diluted 100-fold into buffer A (20 mM Tris-HCl, pH 7.5, 200 mM KCl, 5 mM Mg(OAc)₂), or buffer A containing 0.5 or 1 μM GroEL variants. Aggregation was monitored by light scattering at 320 nm.

Size-exclusion chromatography

Rhodanese, METK or SYT (50 μM each) was denatured for 1 h at 25°C in denaturation buffer and diluted 100-fold into buffer A with or without 0.5 μM GroEL or GroEL-mutants and subjected to gel filtration on a Superdex-200 size-exclusion column (GE Healthcare). Fractions (50 μl) were analysed by SDS-PAGE and immunoblotting for the protein substrates. Fractionation of GroEL was visualized by Ponceau staining. Recoveries of protein substrates were determined by densitometry relative to the loading control.

Analysis of protein solubility *in vivo*

pOFXtac constructs expressing GroEL/GroES or GroEL-mutants/GroES were co-transformed into *E. coli* BL21 cells with the arabinose-controlled expression plasmids for yeast aconitase and WT GFP. Cells were grown in LB medium at 30°C (for GFP expression) and 37°C (for aconitase expression) to an OD₆₀₀ = ~0.5, and chaperonins were induced with 0.1 mM IPTG for 1 h before the induction of substrate proteins with 0.2% arabinose for 2 h. Spheroplasts were prepared and analysed as described (Chang *et al*, 2005). GFP fluorescence was measured in total spheroplast lysates using 96-well plates (20 μg total protein per well) and analysed with a Synergy HT UV/VIS fluorescence plate reader (Bio-Tek) (Chang *et al*, 2005).

In vivo capture of GroEL substrates

GroEL/GroES-substrate complexes were isolated from live *E. coli* spheroplasts co-expressing C-terminally His₆-tagged *M. mazei* GroES (*MmGroES*) and GroEL cavity size-mutants as described previously (Kerner *et al*, 2005). Control pull-downs were performed with lysate expressing WT-GroEL and non-His₆-tagged *MmGroES* to evaluate non-specific binding to the beads. Endogenous substrates contained in chaperonin complexes were detected by immunoblotting.

Fluorescence anisotropy

GFP and DHFR-GFP (25 μM each) was denatured in 6 M GuHCl, 20 mM Tris, pH 7.5, 20 mM KCl and 100-fold diluted into low-salt buffer B (20 mM Tris, pH 7.5, 20 mM KCl, 5 mM Mg(OAc)₂) in the absence or presence of SR-EL variants (1 μM). Encapsulation was achieved by addition of GroES (2 μM), and 5 mM ATP or AMP-PNP, followed by incubation for 30 min at 25°C. Steady-state anisotropy was monitored at the emission wavelength of 508 nm (slit width 5 nm) with an excitation wavelength at 398 nm (slit width 2 nm) using a Fluorolog 3 spectrofluorometer (Spex).

Proteinase K protection of GroEL-GroES-substrate complexes

DHFR-GFP (25 μM) was denatured as above and diluted 100-fold into buffer B in the presence of a fourfold molar excess of SR-EL at 25°C. Reactions were incubated with or without GroES in the presence of 5 mM AMP-PNP for 2 min and treated with proteinase K (2 μg ml⁻¹) for 0–20 min at 25°C (Hayer-Hartl *et al*, 1996; Tang *et al*, 2006). Protease protection of substrate protein was determined by immunoblotting.

In vitro refolding assays

Green fluorescent protein (25 μ M) was denatured in 20 mM Tris, pH 7.5, 20 mM KCl, 6 M GuHCl and refolded upon 100-fold dilution into buffer A or buffer B in the absence or presence of GroEL (0.5 μ M) or SR-EL (1 μ M) as described in the figure legends. Chaperonin-assisted refolding was initiated by the addition of GroES (a twofold molar excess over GroEL or SR-EL) and 5 mM ATP at 25°C. GFP fluorescence was monitored on a Fluorolog 3 Spectrofluorometer (Spex) as described above.

Rhodanese (50 μ M) was denatured in denaturation buffer and refolded upon 100-fold dilution into buffer A or buffer B supplemented with chaperones as indicated in the figure legends and folding was initiated as above. Refolding was stopped at different times by the addition of 50 mM CDTA, followed by colorimetric rhodanese assay (Hayer-Hartl *et al*, 1996).

ATPase assay

GroEL (0.2 μ M oligomer) was incubated in 20 mM Tris-HCl, pH 7.5, 200 mM KCl, 5 mM MgCl₂ for 5 min at 25°C; when indicated, GroES

was present at a twofold molar excess over GroEL. The reaction was initiated by the addition of 2 mM ATP. ATPase activities were followed for 0–20 min, with time points taken every 2.5 min. Reactions were stopped by the addition of 15 mM CDTA. Quantification of liberated inorganic phosphate was measured by the malachite green assay (Lanzetta *et al*, 1979).

Supplementary data

Supplementary data are available at *The EMBO Journal* Online (<http://www.embojournal.org>).

Acknowledgements

We thank D Wischniewski and N Wischniewski for technical assistance with protein purification. Financial support from the Deutsche Forschungsgemeinschaft (SFB 594), the Ernst-Jung Foundation and the Körber Foundation is acknowledged.

References

- Baumketner A, Jewett A, Shea JE (2003) Effects of confinement in chaperonin assisted protein folding: rate enhancement by decreasing the roughness of the folding energy landscape. *J Mol Biol* **332**: 701–713
- Brinker A, Pfeifer G, Kerner MJ, Naylor DJ, Hartl FU, Hayer-Hartl M (2001) Dual function of protein confinement in chaperonin-assisted protein folding. *Cell* **107**: 223–233
- Brocchieri L, Karlin S (2000) Conservation among HSP60 sequences in relation to structure, function, and evolution. *Prot Sci* **9**: 476–486
- Castanié HP, Berges H, Oreglia J, Prère MF, Fayet O (1997) A set of pBR322-compatible plasmids allowing the testing of chaperone-assisted folding of proteins overexpressed in *Escherichia coli*. *Anal Biochem* **254**: 150–152
- Chang HC, Kaiser CM, Hartl FU, Barral JM (2005) *De novo* folding of GFP fusion proteins: high efficiency in eukaryotes but not in bacteria. *J Mol Biol* **353**: 397–409
- Chaudhuri TK, Farr GW, Fenton WA, Rospert S, Horwich AL (2001) GroEL/GroES-mediated folding of a protein too large to be encapsulated. *Cell* **107**: 235–246
- Chen DH, Song JL, Chuang DT, Chiu W, Ludtke SJ (2006) An expanded conformation of single-ring GroEL–GroES complex encapsulates an 86 kDa substrate. *Structure* **14**: 1711–1722
- Farr GW, Fenton WA, Horwich AL (2007) Perturbed ATPase activity and not ‘close confinement’ of substrate in the *cis* cavity affects rates of folding by tail-multiplied GroEL. *Proc Natl Acad Sci USA* **104**: 5342–5347
- Fayet O, Ziegelhoffer T, Georgopoulos C (1989) The GroES and GroEL heat shock gene products of *Escherichia coli* are essential for bacterial growth at all temperatures. *J Bacteriol* **171**: 1379–1385
- Fukuda H, Arai M, Kuwajima K (2000) Folding of green fluorescent protein and the cycle3 mutant. *Biochemistry* **39**: 12025–12032
- Guzman LM, Belin D, Carson MJ, Beckwith J (1995) Tight regulation, modulation, and high-level expression by vectors containing the arabinose p-BAD promoter. *J Bacteriol* **177**: 4121–4130
- Hartl FU, Hayer-Hartl M (2002) Molecular chaperones in the cytosol: from nascent chain to folded protein. *Science* **295**: 1852–1858
- Hayer-Hartl M, Minton AP (2006) A simple semiempirical model for the effect of molecular confinement upon the rate of protein folding. *Biochem* **45**: 13356–13360
- Hayer-Hartl MK, Weber F, Hartl FU (1996) Mechanism of chaperonin action: GroES binding and release can drive GroEL-mediated protein folding in the absence of ATP hydrolysis. *EMBO J* **15**: 6111–6121
- Horwich AL, Fenton WA, Chapman E, Farr GW (2007) Two families of chaperonin: physiology and mechanism. *Ann Rev Cell Develop Biol* **23**: 115–145
- Iwai H, Lingel A, Pluckthun A (2001) Cyclic green fluorescent protein produced *in vivo* using an artificially split PI-PfuI intein from *Pyrococcus furiosus*. *J Biol Chem* **276**: 16548–16554
- Jewett AI, Shea J-E (2008) Do chaperonins boost protein yields by accelerating folding or preventing aggregation? *Biophys J* **94**: 2987–2993 doi:10.1529/biophysj.107.113209
- Kerner MJ, Naylor DJ, Ishihama Y, Maier T, Chang HC, Stines AP, Georgopoulos C, Frishman D, Hayer-Hartl M, Mann M, Hartl FU (2005) Proteome-wide analysis of chaperonin-dependent protein folding in *Escherichia coli*. *Cell* **122**: 209–220
- Lanzetta PA, Alvarez LJ, Reinach PS, Candia OA (1979) An improved assay for nanomole amounts of inorganic phosphate. *Anal Biochem* **100**: 95–97
- Lucent D, Vishal V, Pande VS (2007) Protein folding under confinement: a role for solvent. *Proc Natl Acad Sci USA* **104**: 10430–10434
- Martin J, Langer T, Boteva R, Schramel A, Horwich AL, Hartl FU (1991) Chaperonin-mediated protein folding at the surface of GroEL through a ‘molten globule’-like intermediate. *Nature* **352**: 36–42
- Mayhew M, Da Silva ACR, Martin J, Erdjument-bromage H, Tempst P, Hartl FU (1996) Protein folding in the central cavity of the GroEL–GroES chaperonin complex. *Nature* **379**: 420–426
- McLennan NF, Girshovich AS, Lissin NM, Charters Y, Masters M (1993) The strongly conserved carboxyl-terminus glycine-methionine motif of the *Escherichia coli* GroEL chaperonin is dispensable. *Mol Microbiol* **7**: 49–58
- Paul S, Singh C, Mishra S, Chaudhuri TK (2007) The 69 kDa *Escherichia coli* maltodextrin glucosidase does not get encapsulated underneath GroES and folds through *trans* mechanism during GroEL/GroES-assisted folding. *FASEB J* **21**: 2874–2885
- Rye HS, Burston SG, Fenton WA, Beechem JM, Xu Z, Sigler PB, Horwich AL (1997) Distinct actions of *cis* and *trans* ATP within the double ring of the chaperonin GroEL. *Nature* **388**: 792–798
- Rye HS, Roseman AM, Chen S, Furtak K, Fenton WA, Saibil HR, Horwich AL (1999) GroEL–GroES cycling: ATP and nonnative polypeptide direct alternation of folding-active rings. *Cell* **97**: 325–338
- Takagi F, Koga N, Takada S (2003) How protein thermodynamics and folding mechanisms are altered by the chaperonin cage: molecular simulations. *Proc Natl Acad Sci USA* **100**: 11367–11372
- Tang YC, Chang HC, Roeben A, Wischniewski D, Wischniewski N, Kerner MJ, Hartl FU, Hayer-Hartl M (2006) Structural features of the GroEL–GroES nano-cage required for rapid folding of encapsulated protein. *Cell* **125**: 903–914
- Tehver R, Thirumalai D (2008) Kinetic model for the coupling between allosteric transitions in GroEL and substrate protein folding and aggregation. *J Mol Biol* **377**: 1279–1295
- Thirumalai D, Lorimer GH (2001) Chaperonin-mediated protein folding. *Ann Rev Biophys Biomol Struct* **30**: 245–269
- Wang JD, Herman C, Tipton KA, Gross CA, Weissman JS (2002) Directed evolution of substrate-optimized GroEL/ES chaperonins. *Cell* **111**: 1027–1039
- Weissman JS, Rye HS, Fenton WA, Beechem JM, Horwich AL (1996) Characterization of the active intermediate of a GroEL–GroES-mediated protein folding reaction. *Cell* **84**: 481–490
- Yifrach O, Horovitz A (2000) Coupling between protein folding and allostery in the GroE chaperonin system. *Proc Natl Acad Sci USA* **97**: 1521–1524